PHYSICAL REVIEW B VOLUME 27, NUMBER 12 15 JUNE 1983

Renormalization-group methods for the spectra of disordered chains

Mark O. Robbins and Belita Koiller*
Department of Physics, University of California, Berkeley, California 94720
(Received 18 January 1983)

A family of real-space renormalization techniques for calculating the Green's functions of disordered chains is developed and explored. The techniques are based on a recently proposed renormalization method which is rederived here and shown to be equivalent to a virtual-crystal approximation on a renormalized Hamiltonian. The derivation suggests how other conventional alloy methods can be coupled to the renormalization concept. Various examples are discussed. Short-range order in the occupation of alloy sites and very general disorder in the Hamiltonian—diagonal, off-diagonal, and environmental—are readily incorporated. The techniques are exact in the limits of high and low concentration and of complete short-range order and for the Lloyd model. All states are found to be localized, in agreement with exact treatments. Results for the alloy density of states are presented for various cases and compared to numerical simulations on long chains (10^5 atoms).

I. INTRODUCTION

One-dimensional systems are increasingly of practical as well as theoretical significance. Quasi-one-dimensional materials of current interest[1] include polyacetalene, charge-transfer salts [tetrathiafulvalene-tetracyanoquinodimethane (TTF-TCNQ), etc.], and biological macromolecules.[2] Alloy techniques for calculating the effect of disorder in such systems are of interest in their own right and also provide an approach for treating certain many-body problems.[3] In this paper we develop a family of renormalization methods for calculating the Green's functions of disordered chains and present results for several cases.

The low connectivity of one-dimensional systems has striking consequences for the properties of their eigenstates. Mott and Twose's[4] suggestion that all states should be localized by any disorder has been proved for very general cases.[5] As might be expected from this result, the density of states (DOS) of disordered chains can be highly structured. In the important case of a binary alloy there is an infinite set of exact gaps in the DOS for sufficiently large diagonal disorder.[6,7] Numerical solutions[7] of Schmidt's[8] exact functional equations for the total integrated DOS and simulations on very long chains[9] reveal an intricately detailed spectrum. Both methods give histograms of the number of states in a given energy range Δ. As Δ is decreased, new structure is continually revealed in the DOS.

Although solutions of Schmidt's equations provide a valuable test of analytic approximations, they are difficult to solve numerically, and give little information about the nature of the eigenstates. Localization lengths and the partial DOS on individual species, which determine charge transfer, are not obtained. To our knowledge, Schmidt's exact equations have only been solved in the case of purely diagonal disorder. Numerical simulations in their simplest form give no further information and become expensive if localization lengths and the partial DOS are calculated. These considerations have motivated a great deal of effort towards finding approximate analytic schemes.[10–18]

Traditional single-site approximations[10–14] for the DOS of disordered systems fail badly in one dimension (1D), producing featureless spectra quite unlike the results of numerical simulations.[13] The best conventional single-site method, the coherent-potential approximation[12] (CPA), is a mean-field theory which is correct to lowest order in the reciprocal coordination number Z^{-1}. The CPA is successful in three dimensions where $Z \sim 10$, but not in 1D where $Z = 2$.

Previous attempts[15–18] to improve single-site methods have been aimed at incorporating coherent scattering by small clusters of atoms. This builds in the effect of short-range compositional fluctuations. The resulting spectra correctly capture more of the gross structure in the exact DOS, in particular those peaks corresponding to eigenvalues of clusters of the chosen size. The correlation between the range of fluctuations included in a technique and the degree of structure in the calculated spectrum led Gonçalves da Silva and Koiller[19] to suggest a quali-

 ©1983 The American Physical Society

tatively different approach. The method, based on the renormalization group[20] (RG), treats compositional fluctuations at all length scales equally. The results are striking, all states are localized in the presence of disorder, and the DOS of binary alloys appears to become a set of delta functions with infinitesimal spacing. Subsequent work[21,22] has revealed the versatility of the approach. Short-range order and diagonal, off-diagonal, and environmental disorder in the alloy Hamiltonian can be included[21] without extra computational effort. The method is exact in the limits of complete short-range order (SRO) and high and low concentrations and for the Lloyd model.[23]

The purpose of this paper is to show how conventional alloy averaging techniques can be applied to the renormalization approach of Refs. 19 and 21. Note that this approach is conceptually different from that used in other recent real-space RG calculations[24] for quantum-mechanical systems. These calculations involve projecting the Hamiltonian onto subspaces spanned by eigenvectors of lowest energy. Our method is more closely related to RG decimation techniques[25] for classical systems, where degrees of freedom at different length scales are eliminated successively.

The goal of our renormalization procedure is to calculate the Green's function at one length scale, given the Green's function at a shorter length scale. At the initial length scale, sites along the chain are labeled by consecutive integers. The Green's function G^0 for a particular configuration of species on the chain is expressed in terms of an auxiliary operator O^0: $G^0=\phi(O^0)$. In the examples explicitly developed here, O^0 is the Hamiltonian (Sec. II C) or the scattering t matrix (Sec. II D). An ensemble of chains, specified by a given probability distribution function, is considered. The renormalization proceeds as follows.

(i) The operator G^0 is projected onto even-numbered sites, which are the only sites kept at the new length scale. A new auxiliary operator O' is calculated that gives the projected Green's function G' through the same functional expression connecting G^0 and O^0: $G'=\phi(O')$. No approximation is involved in this step, but the projected quantities still depend on the species at the odd-numbered sites.

(ii) The dependence of G' and the probability distribution function on odd-numbered sites is eliminated by configuration averaging over the occupations of *these sites only.* The configuration average of G' is approximated by $\langle G'\rangle_{\rm odd}\approx G^{(1)}=\phi(O^{(1)})$, where $O^{(1)}\equiv\langle O'\rangle_{\rm odd}$ defines a renormalized auxiliary operator.

(iii) The remaining sites are relabeled by consecutive integers to complete the cycle.

These steps may be iterated to their fixed point for each energy. The alloy DOS is calculated from the fixed points, and localization lengths can be calculated from the asymptotic approach to the fixed points.

The approximation involved in step (ii) of the renormalization procedure is analogous to the approximations made in conventional alloy methods. The Herglotz character of the renormalized Green's function is preserved as it is in the corresponding conventional methods, i.e., the DOS is always positive definite. The difference between the conventional and the RG approaches is that in conventional methods all site occupations are averaged simultaneously, while in RG methods the average is performed sequentially at different length scales.

In Secs. II A and II B of the paper we describe the tight-binding alloy Hamiltonian and the configuration probability distribution function. In Sec. II C we derive a renormalized analog of the virtual-crystal approximation (VCA) and show that it is equivalent to the method of Refs. 19 and 21. A renormalized version of the average—t-matrix approximation (ATA) is developed in II D. The accuracy of conventional alloy methods and their renormalized analogs is compared in II E by examining moments of the calculated DOS. Extensions of the renormalization method and applications of further conventional approximations are briefly discussed in II F. In Sec. III results are presented for the renormalized VCA and ATA. They are compared to the conventional CPA and exact histograms of the DOS of long randomly generated chains (10^5 atoms). Finally, Sec. IV presents a summary and conclusions.

II. FORMALISM

A. Hamiltonian

The equations presented here refer to electronic states. They can be easily modified[13] to treat phonons or magnons. For simplicity, the tight-binding Hamiltonian H^0 is assumed to contain only nearest-neighbor hopping matrix elements and a single orbital per site. Sites are labeled by an integer n, and the species and orbital at site n are denoted by α_n and $|n\rangle$, respectively. The Hamiltonian is then

$$H^0=\sum_n\left[U^0(\alpha_{n-1}\alpha_n\alpha_{n+1})\,|n\rangle\langle n| + \sum_{j=\pm1}V^0(\alpha_n\alpha_{n+j})\,|n\rangle\langle n+j|\right]. \tag{1}$$

Matrix elements U^0 and V^0 depend only on the atomic species at the relevant sites. Off-diagonal elements V^0 are chosen to be real.

If there is environmental disorder (ED), the diagonal element for site n also depends on the occupation of *neighboring* sites,

$$U^0(\alpha_{n-1}\alpha_n\alpha_{n+1})\equiv\epsilon^0(\alpha_n)+s(\alpha_n\alpha_{n-1}) +s(\alpha_n\alpha_{n+1}) \ . \tag{2}$$

In the electronic problem ED can result from chemical shifts or lattice distortions. In phonon and magnon Hamiltonians the diagonal element *necessarily*[13] depends on the types of atom on adjacent sites (except for phonons in the simple case of mass disorder, e.g., two isotopes of the same species).

B. Configuration probabilities

We treat the case of Markovian[17] SRO. The probability distribution for different arrangements of species on the chain is determined completely by pair probabilities $y^0_{\alpha\beta}$. These give the probability that adjacent sites n and $n+1$ are occupied by α and β species, respectively. By symmetry, $y^0_{\alpha\beta}=y^0_{\beta\alpha}$. Any number of species may be considered. In a random alloy, sites are occupied independently, thus $y^0_{\alpha\beta}=c_\alpha c_\beta$, where c_α and c_β are the concentrations of the given species. Other values of $y^0_{\alpha\beta}$ imply differing degrees of correlation in the occupation of neighboring sites, or SRO. For example, $y^0_{\alpha\alpha}=c_\alpha$ implies segregation of species α, and $y^0_{\alpha\beta}=\frac{1}{2}$ corresponds to a strictly alternating chain of α and β atoms.

Markovian SRO is appropriate for a RG method because the distribution function of the chain *after decimation* of alternate sites *remains Markovian.* The new renormalized pair probabilities $y^{(1)}_{\alpha\gamma}$ are calculated by summing over possible occupations β of the decimated site between an α and a γ atom:

$$y^{(1)}_{\alpha\gamma}=\sum_\beta (y^0_{\alpha\beta}y^0_{\beta\gamma}/c_\beta)\equiv R_y[y^0] \ . \tag{3}$$

The concentrations are unchanged. To perform configurational averages over decimated sites in later sections, we need the probability $p^0_{\alpha\beta\gamma}$ that a β atom occupies a site given that the neighbors are an α and a γ atom. This is just

$$p^0_{\alpha\beta\gamma}=(y^0_{\alpha\beta}y^0_{\beta\gamma}c_\beta^{-1})/y^{(1)}_{\alpha\beta} \ . \tag{4}$$

In the results presented in Sec. III we specialize to the case of a binary alloy, $\alpha=A$ or B. Then only two parameters are needed to determine $y_{\alpha\beta}$ because of symmetry and normalization constraints. A convenient[26] parametrization is as follows:

$$\begin{aligned} y^0_{AA}&=x^2+x(1-x)\sigma^0 \ , \\ y^0_{AB}&=y^0_{BA}=x(1-x)(1-\sigma^0) \ , \\ y^0_{BB}&=(1-x)^2+x(1-x)\sigma^0 \ , \end{aligned} \tag{5}$$

where $x=c_A$, and σ^0 is a parameter describing the degree of SRO. As σ^0 varies from $+1$ to -1, the arrangement of atoms on the chain changes from completely *segregated,* all atoms surrounded by like neighbors, to *alternating,* all atoms surrounded by unlike neighbors. For the random alloy $\sigma^0=0$.

The renormalized pair probabilities for the binary alloy are particularly simple. The summation in (3) yields equations for $y^{(1)}_{\alpha\beta}$ with the same form as (5), but with a renormalized SRO parameter $\sigma^{(1)}=[\sigma^0]^2$. At the Nth renormalization step

$$\sigma^{(N)}=[\sigma^{(N-1)}]^2\equiv R_\sigma[\sigma^{(N-1)}] \ . \tag{6}$$

For $|\sigma|\neq 1$ the SRO parameter goes to 0 for large N. Correlations at long length scales go to zero precisely because of the short-range character of Markovian order.

C. Renormalized virtual-crystal method (RVCM)

The simplest alloy technique is the virtual-crystal approximation.[10,14] The configurational average of the Green's function, $G^0(z)=(z-H^0)^{-1}$, is approximated by

$$G_{\rm VCA}(z)=(z-\langle H^0\rangle_{\rm all})^{-1} \ , \tag{7}$$

where the indicated configuration average is over all sites. The corresponding renormalization technique is generated by taking the Hamiltonian as the auxiliary operator discussed in Sec. I.

The equation for the Green's function at the original length scale can be expanded as

$$G^0(z)=z^{-1}\sum_{j=0}^{\infty}(H^0/z)^j \ , \tag{8}$$

The projected Green's function and the auxiliary operator H' are related in the same way:

$$G'\equiv P_{\rm even}G^0=z^{-1}\sum_{j=0}^{\infty}(H'/z)^j \ , \tag{9}$$

where $P_{\rm even}=\sum_n |2n\rangle\langle 2n|$.

To calculate H' it is convenient to introduce a diagram notation. The identity, $\sum_n |n\rangle\langle n|$, is inserted around each factor of H^0/z in (8). The matrix elements of G^0 are then expressed in terms of a series of products of matrix elements of H^0: $H^0_{mn}=\langle m|H^0|n\rangle$. Successive matrix elements of

H^0 in a product must share a common orbital, e.g., $\cdots H^0_{mn}H^0_{np}H^0_{pq}\cdots$. As a bookkeeping measure, each matrix element H^0_{mn} is associated with a step along the alloy chain from site m to site n. Then each contribution to $(H^0/z)^j$ corresponds to a continuous j step path or "diagram" on the chain. The magnitude of the path's contribution to $(H^0/z)^j$ is the product of the matrix elements associated with each step, divided by z^j. For a tight-binding Hamiltonian with nearest-neighbor hopping, each step can only change the index by 0 or ± 1. The paths contributing to $\langle 2n \mid G \mid 2n \rangle$ from $(H^0/z)^3$ are illustrated in Fig. 1.

From (9), $P_{\text{even}}H'=H'$. For the renormalization concept to be applicable, H' should have the same form as H^0 but on a new length scale, i.e., $\langle 2m \mid H' \mid 2n \rangle$ should be nonzero only if $\mid m-n \mid =0,1$. The conditions on H' are satisfied if its matrix elements are calculated by summing the diagrams indicated in Fig. 2. These are all the paths in G^0, associated with factors of H^0, which contain only odd-numbered *intermediate* sites. All other

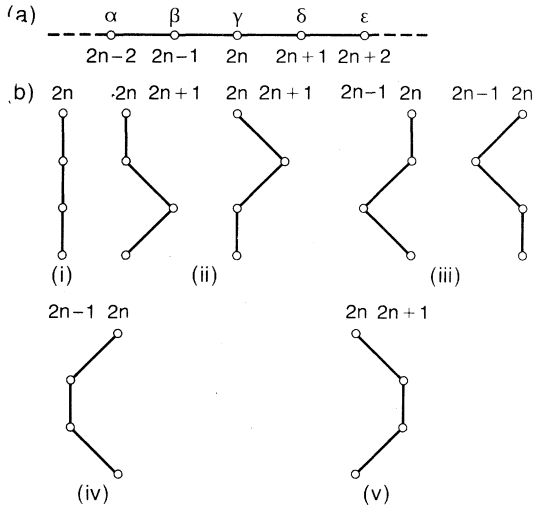

FIG. 1. Illustration of the diagrammatic notation for terms in expansion (8). (a) Relevant section of the chain: Site labels are given below and atomic species above each site. (b) Paths contributing to $\langle 2n \mid G^0 \mid 2n \rangle$ from $(H^0/z)^3$. Movement along the chain is indicated by horizontal displacements while downward displacements separate successive steps. Site indices are indicated above each diagram. The contribution of each path to $z\langle 2n \mid G^0 \mid 2n \rangle$ is as follows: (i) $[U^0(\beta\gamma\delta)/z]^3$; (ii) $[U^0(\beta\gamma\delta)/z][V^0(\gamma\delta)/z]^2$; (iii) $[U^0(\beta\gamma\delta/z][V^0(\beta\gamma)/z]^2$; (iv) $[V^0(\beta\gamma)/z]^2[U^0(\alpha\beta\gamma)/z]$; (v) $[V^0(\gamma\delta)/z]^2 \times[U^0(\gamma\delta\epsilon)/z]$.

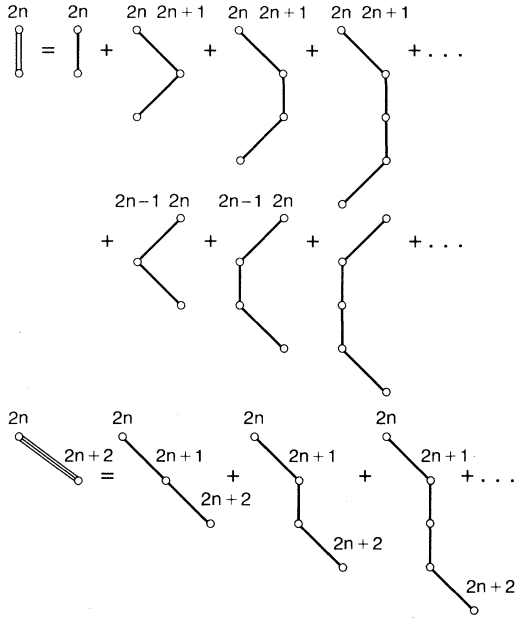

FIG. 2. Diagrams contributing to the matrix elements of H'. Upper diagrams: $z^{-1}\langle 2n \mid H' \mid 2n \rangle$. Lower diagrams: $z^{-1}\langle 2n \mid H' \mid 2n+2 \rangle$.

paths contributing to G' are incorporated exactly in (9) through higher-order terms in H'.

The summation, illustrated in Fig. 2, is easily performed by grouping terms into geometric series. We find

$$\begin{aligned}\langle 2n \mid H' \mid 2n \rangle &= U^0(\beta\gamma\delta) \\ &\quad +[V^0(\gamma\beta)]^2[z-U^0(\alpha\beta\gamma)]^{-1} \\ &\quad +[V^0(\gamma\delta)]^2[z-U^0(\gamma\delta\epsilon)]^{-1} \quad , \qquad (10) \\ \langle 2n-2 \mid H' \mid 2n \rangle &= V^0(\alpha\beta)V^0(\beta\gamma)[z-U^0(\alpha\beta\gamma)]^{-1} \quad ,\end{aligned}$$

where α, β, γ, δ, and ϵ are, respectively, the species at sites $2n-2$ through $2n+2$ as in Fig. 1(a). At this point, step (i) of the renormalization procedure is complete.

The approximate configuration average of G', step (ii) in the renormalization procedure, is

$$\langle G' \rangle_{\text{odd}} \simeq G^{(1)} \equiv z^{-1}\sum_{j=0}^{\infty}(H^{(1)}/z)^j \quad , \qquad (11)$$

with $H^{(1)}=\langle H' \rangle_{\text{odd}}$. The configurational average of H' is easily performed using the results of Sec. II B. From (4) and (10) the diagonal and off-diagonal elements, $U^{(1)}$ and $V^{(1)}$, of the renormalized Hamil-

tonian $H^{(1)}$ are as follows:

$$U^{(1)}(\alpha\gamma\epsilon)=\sum_{\beta,\delta} p^0_{\alpha\beta\gamma}p^0_{\gamma\delta\epsilon}\left[U^0(\beta\gamma\delta)+\frac{[V^0(\gamma\beta)]^2}{z-U^0(\alpha\beta\gamma)}+\frac{[V^0(\gamma\delta)]^2}{z-U^0(\gamma\delta\epsilon)}\right]$$

$$\equiv R_U[z,y^0,U^0,V^0] \ ,$$

$$V^{(1)}(\alpha\gamma)=\sum_{\beta} p^0_{\alpha\beta\gamma}V^0(\alpha\beta)V^0(\beta\gamma)[z-U^0(\alpha\beta\gamma)]^{-1}$$

$$\equiv R_V[z,y^0,U^0,V^0] \ . \tag{12}$$

The functions R_y, R_U, and R_V in (3) and (12) define recursion relations for the renormalization procedure that may be iterated numerically. For $z=E+i\eta$, $\eta>0$, the fixed point of R_V is $R_V^\infty=0$. The fixed point of R_U depends only on the central species γ:

$$U^\infty_\gamma(z)\equiv U^\infty(\alpha,\gamma,\epsilon) \ . \tag{13}$$

The simple form of the Hamiltonian at the fixed point allows us to calculate the average local DOS on a γ atom. By definition

$$\rho_\gamma(E)\equiv-\pi^{-1}\lim_{\eta\to0+}\mathrm{Im}\langle G^\gamma_{00}(z)\rangle, \quad z=E+i\eta \tag{14}$$

where $\langle G^\gamma_{00}(z)\rangle$ is the configuration average of the diagonal element of G^0 subject to the constraint $\alpha_0=\gamma$. In the RVCM

$$\rho_\gamma(E)=-\pi^{-1}\lim_{\eta\to0+}\mathrm{Im}[z-U^\infty_\gamma(z)]^{-1} \ . \tag{15}$$

The total average DOS is then

$$\rho(E)=\sum_\gamma c_\gamma\rho_\gamma(E) \ . \tag{16}$$

The same expressions [(10), (12)–(16)] were obtained in Ref. 21 by identifying the coefficients of decimated Green's-function equations with the matrix elements of a renormalized Hamiltonian. The matrix elements were then configuration averaged independently in the Green's-function equations. It is evident from our derivation here that this method is equivalent to a VCA on the renormalized Hamiltonian $H^{(1)}$.

The first term in (11) which is not averaged correctly is second order in H':

$$\langle H'^2\rangle\neq\langle H'\rangle^2 \ . \tag{17}$$

The error comes from successive matrix elements depending on the occupation of the *same* decimated site on the right-hand side of (17). In a VCA scheme these matrix elements are averaged *independently*. The average–t-matrix approximation[11,14] (ATA) was developed to overcome this deficiency. In the ATA, all consecutive terms depending on the *same* site occupation are summed exactly into a "t matrix" *before* configuration averaging. This approach can be applied within a renormalization framework.

D. Renormalized average–t-matrix method (RATM)

In the conventional ATA,[11,14] the Hamiltonian is divided into two components:

$$H^0=\tilde{H}+\delta H \ . \tag{18a}$$

The operator $\tilde{H}$ is independent of all site occupations (usually $\tilde{H}=\langle H^0\rangle=H_{\mathrm{VCA}}$), and the disordered part of the Hamiltonian is separated into contributions from each individual site

$$\delta H=\sum_n \delta H_n \ . \tag{18b}$$

The Green's function can be expanded in terms of $\tilde{G}\equiv[z-\tilde{H}]^{-1}$, which is translationally invariant and easily calculated, and δH:

$$G^0=[z-H^0]^{-1}=\tilde{G}+\tilde{G}\,\delta H\,\tilde{G}+\tilde{G}\,\delta H\,\tilde{G}\,\delta H\,\tilde{G}+\cdots \ . \tag{19}$$

All consecutive scattering by δH_n in (19) can be grouped together and summed exactly, defining t matrices:

$$t_n\equiv\delta H_n+\delta H_n\,\tilde{G}\,\delta H_n+\delta H_n\,\tilde{G}\,\delta H_n\,\tilde{G}\,\delta H_n+\cdots \ . \tag{20}$$

In terms of these operators, the Green's function is

$$G^0=\tilde{G}+\tilde{G}\sum_n t_n\tilde{G}+\tilde{G}\sum_n t_n\tilde{G}\sum_{m\neq n} t_m\tilde{G}+\cdots \ . \tag{21}$$

Summations in (21) are restricted to preclude successive factors of the same t_n: All successive scattering by site n is already included in the t matrix. The approximate average Green's function is obtained in the ATA by configuration averaging each t matrix in (21) independently,

$$G_{\mathrm{ATA}}=\tilde{G}+\tilde{G}\sum_n\langle t_n\rangle\tilde{G}+\tilde{G}\sum_n\langle t_n\rangle\tilde{G}\sum_{m\neq n}\langle t_m\rangle\tilde{G}+\cdots \ . \tag{22}$$

The renormalized average—t-matrix method proceeds in an analogous fashion. It is convenient to divide the Hamiltonian as in (18), but taking

$$\tilde{H}^0=\sum_n \epsilon^0(\alpha_n)\,|\,n\,\rangle\langle\,n\,|\ , \tag{23a}$$

$$\begin{aligned}\delta H_n \equiv & s(\alpha_n\alpha_{n+1})\,|\,n\,\rangle\langle\,n\,|+V^0(\alpha_n\alpha_{n+1})\,|\,n\,\rangle\langle\,n+1\,| \\ & +V^0(\alpha_{n+1}\alpha_n)\,|\,n+1\,\rangle\langle\,n\,| \\ & +s(\alpha_{n+1}\alpha_n)\,|\,n+1\,\rangle\langle\,n+1\,|\ ,\end{aligned} \tag{23b}$$

where ϵ^0 and s are defined in (2). The disorder in δH_n is associated with the "bond" connecting sites n and $n+1$. The motivation for this choice is that after a decimation each new "bond" from $2n$ to $2n+2$ is associated with a single decimated site, $2n+1$.

The auxiliary operators in the RATM are the t matrices t_n^0, defined by (20) and (23). The Green's function $\tilde{G}^0$, which enters (20), is

$$\tilde{G}^0=[z-\tilde{H}^0]^{-1}=\sum_n [z-\epsilon^0(\alpha_n)]^{-1}\,|\,n\,\rangle\langle\,n\,|\ . \tag{24}$$

The t matrices are calculated in Appendix A. We find

$$\begin{aligned}t_n^0=&a^0(\alpha_n\alpha_{n+1})\,|\,n\,\rangle\langle\,n\,|+b^0(\alpha_n\alpha_{n+1})\,|\,n\,\rangle\langle\,n+1\,| \\ &+b^0(\alpha_{n+1}\alpha_n)\,|\,n+1\,\rangle\langle\,n\,| \\ &+a^0(\alpha_{n+1}\alpha_n)\,|\,n+1\,\rangle\langle\,n+1\,|\ ,\end{aligned} \tag{25}$$

where the coefficients are as follows:

$$\begin{aligned}a^0(\alpha\beta)=&[z-\epsilon^0(\alpha)]\{s(\alpha\beta)[z-\epsilon^0(\beta)-s(\beta\alpha)] \\ &+[V^0(\alpha\beta)]^2\}/f(\alpha\beta)\ , \\ b^0(\alpha\beta)=&[z-\epsilon^0(\alpha)][z-\epsilon^0(\beta)]V^0(\alpha\beta)/f(\alpha\beta)\ ,\end{aligned} \tag{26}$$

and

$$\begin{aligned}f(\alpha\beta)=&[z-\epsilon^0(\alpha)-s(\alpha\beta)][z-\epsilon^0(\beta)-s(\beta\alpha)] \\ &-[V^0(\alpha\beta)]^2\ .\end{aligned}$$

In order to perform step (i) of the renormalization procedure we must find operators $\tilde{G}'$ and t' which give the projected Green's function through a relation equivalent to (21):

$$\begin{aligned}G'=&P_{\text{even}}G^0 \\ =&\tilde{G}'+\tilde{G}'\sum_n t'_{2n}\tilde{G}' \\ &+\tilde{G}'\sum_n t'_{2n}\tilde{G}'\sum_{m\neq n} t'_{2m}\tilde{G}+\cdots\ .\end{aligned} \tag{27}$$

These new operators should have the same form as $\tilde{G}^0$ and t^0, but on the new length scale. Moreover, $\tilde{G}'$ cannot depend on the occupations of any decimated sites, or the average indicated in (22) is inapplicable. The above conditions are satisfied if

$$\tilde{G}'=P_{\text{even}}\tilde{G}^0\ , \tag{28}$$

and t'_{2n} contains all combined scattering by the two "old bonds" connecting sites $2n$ to $2n+1$ and $2n+1$ to $2n+2$, i.e.,

$$\begin{aligned}t'_{2n}=P_{\text{even}}\sum_{m=0,1}(&t^0_{2n+m}+t^0_{2n+m}\tilde{G}^0t^0_{2n+1-m} \\ &+t^0_{2n+m}\tilde{G}^0t^0_{2n+1-m}\tilde{G}^0t^0_{2n+m} \\ &+\cdots)\ .\end{aligned} \tag{29}$$

To complete step (ii) of the renormalization procedure, $G^{(1)}$ is calculated from (27) by averaging the t matrix as in (22):

$$\begin{aligned}G^{(1)}\approx&\langle G'\rangle_{\text{odd}} \\ =&\tilde{G}^{(1)}+\tilde{G}^{(1)}\sum_n t^{(1)}_{2n}\tilde{G}^{(1)} \\ &+\tilde{G}^{(1)}\sum_n t^{(1)}_{2n}\tilde{G}^{(1)}\sum_{m\neq n} t^{(1)}_{2m}\tilde{G}^{(1)}+\cdots\ ,\end{aligned} \tag{30}$$

where $\tilde{G}^{(1)}=\tilde{G}'$ and the $t^{(1)}_{2n}\equiv\langle t'_{2n}\rangle_{\text{odd}}$ are calculated in Appendix B using Eqs. (23)—(26) and (29). The result can be expressed in terms of recursion relations for the coefficients of the t matrix $a^{(N)}$ and $b^{(N)}$, defined in (25) for $N=0$. These are

$$\begin{aligned}a^{(N+1)}(\alpha\gamma)=&\sum_\beta p^{(N)}_{\alpha\beta\gamma}\{a^{(N)}(\alpha\beta)+[b^{(N)}(\alpha\beta)]^2a^{(N)}(\beta\gamma)/d^{(N)}(\alpha\beta\gamma)\}\ , \\ b^{(N+1)}(\alpha\gamma)=&\sum_\beta p^{(N)}_{\alpha\beta\gamma}\,b^{(N)}(\alpha\beta)b^{(N)}(\beta\gamma)[z-\epsilon^0(\beta)]/d^{(N)}(\alpha\beta\gamma)\ ,\end{aligned} \tag{31a}$$

where

$$d^{(N)}(\alpha\beta\gamma)=[z-\epsilon^0(\beta)]^2-a^{(N)}(\beta\alpha)a^{(N)}(\beta\gamma)\ , \tag{31b}$$

and the $p^{(N)}_{\alpha\beta\gamma}$ are renormalized probabilities defined in (4).

As in the RVCM, the Green's function at the fixed point of the RATM (31) is diagonal for $\eta = \mathrm{Im}(z) > 0$. As $N \to \infty$, $b^{(N)}(\alpha\beta) \to 0$ and $a^{(N)}(\alpha\beta) \to a^{\infty}_{\alpha}$. The configuration average of the diagonal element of the Green's function on an α atom, $\langle G^{\alpha}_{00} \rangle$, is easily calculated at the fixed point from (30). In the RATM

$$\langle G^{\alpha}_{00}(z) \rangle = [z - \epsilon^0(\alpha)]^{-1} \left[1 + 2 \sum_{m=1}^{\infty} \left[\frac{a^{\infty}_{\alpha}}{z - \epsilon^0(\alpha)} \right]^m \right]$$

$$= [z - \epsilon^0(\alpha)]^{-1} \frac{z - \epsilon^0(\alpha) + a^{\infty}(\alpha)}{z - \epsilon^0(\alpha) - a^{\infty}(\alpha)} \quad . \quad (32)$$

The partial DOS on an α species and the total average DOS follow immediately from (14) and (16).

E. Moments

One measure of the quality of an alloy approximation is the number of moments of the DOS that it reproduces exactly. The Mth moment of the DOS, $\rho_n(E)$, projected onto the nth site is defined[27] to be

$$\mu^n_M \equiv \int E^M \rho_n(E) dE = \langle \langle n \mid H^M \mid n \rangle \rangle_{\mathrm{all}} \quad , \quad (33)$$

where the configuration average is over occupations of all sites. The right-hand side of (33) implies that only M-step paths contibute to μ^n_M. Thus low-order moments reflect the influence of *local* properties on the electronic spectrum.

For the case of purely diagonal disorder, Fig. 3 illustrates the shortest paths contributing to the total DOS which are averaged incorrectly by conventional single-site methods[28] and their renormalized analogs. The highest moment of the average DOS which is reproduced exactly is indicated for each method in Table I. The renormalization techniques reproduce substantially more moments than their conventional counterparts. Many diagrams are summed in the initial projection onto even-numbered sites [step (i)] *before* configuration averaging. In the RVCM these diagrams include as a subset all those summed in the conventional ATA. The RATM sums a different set of diagrams than the CPA, but reproduces the same number of moments of the total DOS and one more moment of the partial DOS. For purely diagonal disorder, the first error is second order in the strength of disorder for the RATM and fourth order for the CPA. Therefore the RATM should be more accurate than the

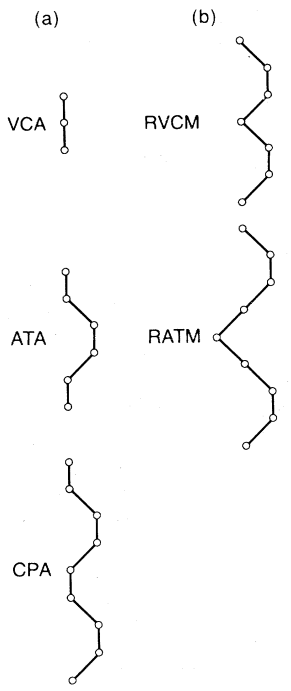

FIG. 3. The shortest paths contributing to the total DOS which are averaged incorrectly by conventional approximations (a), and their renormalized analogs (b), for purely diagonal disorder.

TABLE I. Order of the highest moment of the total DOS reproduced exactly by various alloy techniques for the indicated type of disorder. Numbers in parentheses refer to the highest exact moment of the *partial* DOS, when it is different.

Averaging technique		Disorder: Diagonal	Off-diagonal	Environmental
VCA	Conventional	1	1	1
	Renormalized	5	3	1
ATA	Conventional	4(3)	1	1
	Renormalized	7	5	3
CPA	Conventional	7(6)	3	3

CPA for large disorder.

Table I also indicates the highest moment reproduced exactly by each method in the cases of pure off-diagonal disorder (ODD) and pure environmental disorder (ED). As above, the renormalized methods represent a substantial improvement over their conventional counterparts. The accuracy of all methods decreases as the type of disorder changes from diagonal to off-diagonal to environmental. Note that the conventional CPA and ATA can only be applied to special types[13,14] of ODD and ED: separable, $V_{AB}=\sqrt{V_{AA}V_{BB}}$, or additive, $s_{AB}=(s_{AA}+s_{BB})/2$. Blackman, Esterling, and Berk[29] have extended the CPA to incorporate general ODD. No single-site technique for general ED has been found, but it can be included in the recently developed traveling cluster method.[18] All renormalization methods presented in this paper can include general ODD and ED as well as SRO.

High-order moments are crucial in determining the exact nature of the DOS.[14] These are the moments affected by the long-range fluctuations in occupation that our renormalization methods were designed to include. The marked difference in the nature of spectra calculated with conventional single-site methods and with their renormalized analogs (Sec. III) reflects changes in the treatment of these high-order moments.

F. Extensions and improvements

An obvious way of improving either the RVCM or the RATM is to decimate the chain i times before configuration averaging. Then all paths on the 2^i-1 decimated sites between a *given pair* of neighboring preserved sites are averaged *exactly*. The calculated DOS improves, as illustrated in Sec. III. However, the exact DOS is not obtained in the limit $i\rightarrow\infty$. The values of moments of the DOS improve, but the number of exactly reproduced moments remains constant. The paths indicated in Fig. 3 which give the first incorrect contributions to moments of the DOS in the RVCM and RATM are averaged in the same way for all i. Of course, other diagrams of the same order are averaged correctly for $i>1$. In the numerical examples we compare results for $i=1$, single decimation (SD), and $i=2$, double decimation (DD).

A second class of improved methods is based on more sophisticated averaging techniques than the ATA and VCA. The most straightforward are early cluster generalizations[13-18,30] of single-site methods. The alloy chain is divided into clusters of j atoms each. The RVCM or RATM is then applied, treating the different cluster types as new "atomic species." The number of exact moments increases because all paths within each cluster are averaged exactly. Up to jth nearest-neighbor hopping matrix elements on the chain are mapped into nearest-neighbor hopping elements between clusters. The difficulties in this method are increased computation and, possibly, ambiguous interpretation, because the division into clusters is artificial. Every site in the chain is equivalent, however, approximations in the configuration averaging may lead to inequivalent projected DOS on different sites in the cluster. We have not explored this possibility, but such problems are known to arise[30] in cluster generalizations of conventional methods. The usual solution is to average properties over all cluster sites, or to choose some site as most representative and calculate its DOS.

The development of renormalized analogs of the VCA and ATA suggests that a renormalized version of the CPA should exist. The CPA improves on the ATA by including self-consistently in the t matrix for each site the average scattering from all other sites. In the conventional ATA an arbitrary zero of energy can be chosen for the diagonal elements of the unperturbed Hamiltonian. The CPA was originally derived[12] by finding relations for the optimum choice of this reference energy. A similar degree of freedom exists in the renormalized ATA. An arbitrary energy and species-dependent self-energy can be added to $\tilde{H}^0$ and subtracted from δH in (23). Proper choice of this self-energy may lead to a renormalized analog of the CPA. Research in this direction is in progress.

III. NUMERICAL RESULTS AND DISCUSSIONS

In the numerical examples we specialize to a binary alloy with no environmental disorder. The tight-binding Hamiltonian is characterized by two on-site energies U_A^0 and $U_B^0=U_A^0-\delta V$, where $V=V_{AB}^0=V_{BA}^0$. The off-diagonal matrix elements are taken to be related by $V_{AA}^0=tV_{BB}^0=\sqrt{t}\,V$. Diagonal and off-diagonal disorders are characterized, respectively, by the dimensionless parameters δ and t. Composition and SRO are specified by x and σ as described in Sec. II B.

To provide a standard for the success of our renormalization techniques, we compare our results to the CPA and to numerical evaluations of the DOS of randomly generated Markovian chains with 10^5 atoms. The integrated number of states in successive energy intervals of width Δ was determined by a node-counting technique.[31] For the purpose of our discussion, the resulting histogram of the DOS may be considered an exact average total DOS. Increasing the number of atoms in the chains to 10^6 pro-

duced negligible change for the examples plotted here.

The DOS [Eq. (14)] is given by the imaginary part of $\langle 0 | G(E+i\eta) | 0 \rangle$ in the limit $\eta \rightarrow 0+$. This limit is difficult to calculate or plot because of the pathological analytic character of the spectra of 1D binary alloys. In the results for the DOS presented here we plot

$$\rho(E) = -\pi^{-1} \mathrm{Im} \langle 0 | G(E+i\eta) | 0 \rangle \tag{34}$$

evaluated at a small positive value of η. This is equivalent to convoluting the true DOS with a Lorentzian of half-width η. The value of η is chosen to provide a resolution of features in the DOS which is comparable to the resolution Δ in the exact histogram. The effect of η and Δ and the nature of the spectra of disordered chains are illustrated in Fig. 5 and discussed below.

In Fig. 4 we compare the results of several methods for the total average DOS of a random binary chain with purely diagonal disorder; $\delta=4$, $t=1$. The concentration is $x=0.5$ and the energy resolutions are $\eta=0.02V$ and $\Delta=0.05V$. The exact histogram for the DOS of a long chain and the CPA DOS are compared in 4(c). The CPA spectrum covers roughly the correct energy range, and a gap is present at $E=0$ which is also found in the histogram. However, the gap is too large, and the CPA fails to reproduce any of the other structure in the exact DOS.

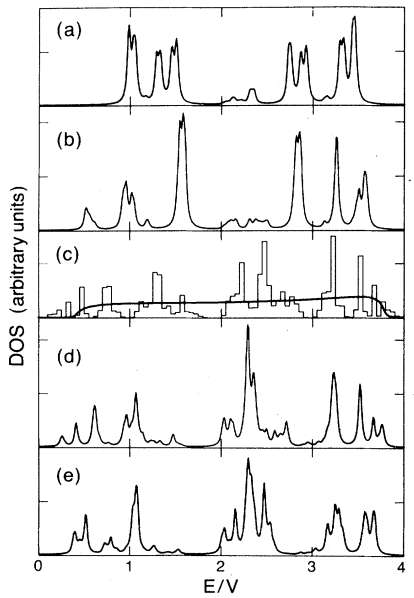

FIG. 4. Results for the total DOS of a random binary chain with purely diagonal disorder: (a) SD-RVCM; (b) DD-RVCM; (c) CPA (thick line) and exact histogram (thin line); (d) DD-RATM; (e) SD-RATM. The parameters, defined in the text, are $\delta=4$, $t=1$, $x=0.5$, $\sigma=0$, and $\eta=0.02V$ (for analytic methods) or $\Delta=0.05V$ (for numerical histogram). The DOS is symmetric, $\rho(E)=\rho(-E)$.

The DOS produced by the RVCM of Refs. 19 and 21 is shown in Fig. 4(a). Some of the structure in the exact DOS is reproduced, but the spectrum is not in good overall agreement with the numerical results. The double decimation version of the RVCM (Sec. II F) gives the spectrum in 4(b). With respect to 4(a), the widths of the gaps at $E=0$ and $E=2V$ are decreased towards the exact values and the position of the upper band edge is improved. Agreement of the peak positions and intensities with those in the exact spectrum is still poor.

The results of the RATM [Figs. 4(d) and 4(e)] represent a striking improvement. The DD-RATM [Fig. 4(d)] in particular reproduces the morphology (the sequence of peaks and their relative heights) of the histogram very well. However, peaks are somewhat shifted from their correct positions ($\lesssim 0.2V$). Shifts in large peaks and peaks at high-energy values are smallest. These are the peaks which contribute most to moments of the DOS.

The difference between the DOS calculated via renormalization methods and the CPA reflects differences in the treatment of compositional fluctuations. The renormalization procedure incorporates fluctuations at all length scales. Scattering between species at one length scale is mediated by an effective field that includes fluctuations at shorter length scales. Approximations involved in calculating this effective field cause the shifts in structure discussed above.

All the renormalization methods presented here yield exact results in the ordered limits, $\sigma=\pm 1$. The random case, $\sigma=0$, considered in Fig. 4 is the least favorable one, and agreement with exact results improves as $|\sigma|$ increases. This is illustrated in Fig. 5 where DD-RATM results [Figs. 5(a) and 5(c)] are compared to exact histograms [Figs. 5(b) and 5(d)] for $\sigma=-0.5$ (tendency to form a binary chain) and $\delta=4$. As in Fig. 4 the DD-RATM reproduces the morphology of the DOS very well. Note that shifts in the peak positions are generally smaller than in Fig. 4 because of the ordering.

Figure 5 also illustrates the rich structure in the DOS of binary alloy chains. The calculation for Figs. 5(a) and 5(b) was repeated with the energy resolution increased by a factor of 5. Both the exact histogram [Fig. 5(d)] and the DD-RATM [Fig. 5(c)] results show finer structure which was unresolved at the previous values of Δ and η. The qualitative agreement between the two methods is maintained. New structure continues to be found[7] as the resolu-

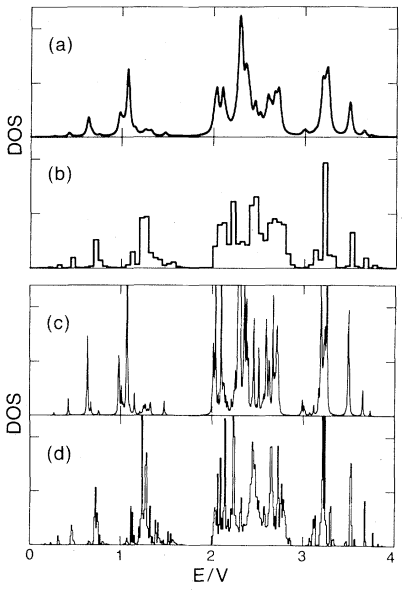

FIG. 5. Calculated DOS for the chain of Fig. 4 with partial order, $\sigma=-0.5$, and two different energy resolutions: (a) DD-RATM, $\eta=0.02V$, (b) exact histogram, $\Delta=0.05V$, (c) DD-RATM, $\eta=0.004V$, and (d) exact histogram, $\Delta=0.01V$.

tion is further increased. Conventional analytic methods do not exhibit this behavior, even if one goes beyond the single-site approximation, because they are mean-field techniques.

The extreme structure in the DOS of Figs. 4 and 5 is associated with short localization lengths. The inverse localization length K may be defined in terms of the decay of off-diagonal matrix elements of G at large distance:

$$K=-\lim_{N\to\infty} N^{-1}\langle \ln G_{2N,0}-\ln G_{N,0}\rangle_{\text{all}} . \tag{35}$$

For $\eta>0$, the Green's function is always diagonal at the fixed points of the renormalization methods presented here: $G_{N,0}(z)\to 0$ as $N\to\infty$. In disordered chains the fixed point *remains* diagonal in the limit $\eta\to 0$. *All states are localized.* The rate of convergence to the fixed point gives an approximate inverse localization length. Only in completely ordered chains does this inverse localization length diverge.

From the above discussion it is evident that the number of iterations required to reach the fixed point in numerical evaluations of the DOS depends on two factors: the size of η and the inverse localization length. For the ordered chain the number of iterations diverges as $\eta\to 0$, but is only ~ 10 for the value $\eta=0.02V$. For disordered chains, the number of iterations saturates as $\eta\to 0$ at a value N given approximately by $2^N\sim K^{-1}$. A complete discussion of the application of renormalization methods to the study of localization will be reported elsewhere.

In Fig. 6 we plot the average DOS for a random binary chain with off-diagonal disorder only; $t=2$, $\delta=0$. The other parameters are $\sigma=0$, $x=0.5$, $\eta=0.015V$, and $\Delta=0.035V$. Results from the DD versions of the RVCM and RATM are compared to the exact histogram. The DOS's given by all methods are flat for values of E near 0. Both pure elements have states in this energy region. As E increases structure develops. The RVCM produces spurious structure at intermediate energies ($0.7V<|E|<1.4V$) and does not reproduce the structure in the histogram at higher energies. The RATM provides much better agreement. Less spurious structure is present at intermediate energies (see, however, the peak at $E=1.3V$). As in the case of diagonal disorder, the morphology of the peaks at higher energy is reproduced but at somewhat shifted positions. The agreement is not quite as good as in the case of diagonal disorder, because the number of exact moments is lower when off-diagonal disorder is present.

IV. SUMMARY AND CONCLUSIONS

We have presented a systematic study of applications of the RG procedure and conventional alloy averaging techniques to the calculation of the DOS of 1D disordered systems. A previously suggested method[19,21] was rederived as a virtual-crystal approximation on a renormalized Hamiltonian, and

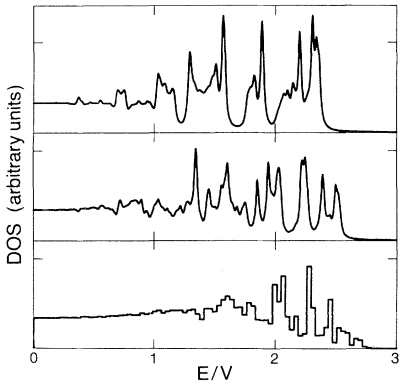

FIG. 6. Average DOS for a random binary chain with purely off-diagonal disorder. From top to bottom: results from DD-RVCM, DD-RATM, and exact histogram. The parameters, defined in the text, are $t=2$, $x=0.5$, $\sigma=0$, $\eta=0.015V$, and $\Delta=0.035V$. The DOS is symmetric $\rho(E)=\rho(-E)$.

extended via multiple-decimation techniques. A renormalized version of another conventional single-site approach—the ATA—was derived and shown to constitute a substantial improvement over the renormalized virtual-crystal method. Other applications were suggested.

Generalizations of the renormalization methods to higher dimension are desirable. Compositional fluctuations are less important in two and three dimensions, but still dominate the question of localization. Unfortunately, the methods described here are not directly applicable to lattices with higher connectivity than a chain. Traditional approximations[32] for 2D RG calculations may prove fruitful, but will not yield the exact DOS in ordered limits. However, chains of finite width in two or three dimensions may be readily treated.

The renormalization methods described here represent a dramatic improvement over their conventional counterparts. Some discrepancies remain between the renormalized ATA and the exact DOS, but we believe the RG approach is a promising route to better approximations for the properties of disordered chains. The computational simplicity of these methods, and their ability to incorporate very general types of disorder in a natural manner, encourage research based on more sophisticated conventional alloy methods. The fact that all states are found to be localized with easily calculable localization lengths is an especially desirable feature for treatments of disordered chains.

ACKNOWLEDGMENTS

We thank L. M. Falicov for useful comments, T. Kaplan for providing a program for the DOS of long chains, and M. Gabay and C. E. T. Gonçalves de Silva for interesting conversations. Support from the National Science Foundation through Grant No. DMR-81-06494 is gratefully acknowledged. One of us (B.K.) acknowledges support from the Guggenheim Foundation and from the Brazilian agencies Financiadora de Estudos e Projetos (FINEP) and Conselho Nacional de Pesquisa do Brasil (CNPq).

APPENDIX A

The t matrices are given by

$$t_n^0=\delta H_n+\delta H_n\tilde{G}^0\delta H_n+\delta H_n\tilde{G}^0\delta H_n\tilde{G}^0\delta H_n+\cdots\ , \tag{A1}$$

where δH_n and $\tilde{G}^0$ are defined in (23b) and (24). The summation is simplified if the diagonal and off-diagonal components of δH_n are considered separately. The diagonal terms are incorporated in a new operator g_n

$$g_n\equiv[z-\lambda(\alpha_n\alpha_{n+1})]^{-1}\,|\,n\,\rangle\langle\,n\,|\\ +[z-\lambda(\alpha_{n+1}\alpha_n)]^{-1}\,|\,n+1\,\rangle\langle\,n+1\,|\ , \tag{A2}$$

where $\lambda(\beta\gamma)\equiv\epsilon^0(\beta)+s(\beta\gamma)$, and the off-diagonal terms in

$$\delta h_n\equiv V^0(\alpha_n\alpha_{n+1})\,|\,n\,\rangle\langle\,n+1\,|\\ +V^0(\alpha_{n+1}\alpha_n)\,|\,n+1\,\rangle\langle\,n\,|\ . \tag{A3}$$

Equation (A1) can be rewritten as

$$[(\tilde{G}^0)^{-1}-\delta H_n]\tilde{G}^0t_n^0=\delta H_n\ . \tag{A4}$$

By regrouping terms on the left we find

$$[g_n^{-1}-\delta h_n]\tilde{G}^0t_n^0=\delta H_n\ , \tag{A5}$$

and thus

$$t_n^0=(\tilde{G}^0)^{-1}q_n\delta H_n\ , \tag{A6}$$

where

$$q_n\equiv(1-g_n\delta h_n)^{-1}g_n\\ =(1+g_n\delta h_n+g_n\delta h_ng_n\delta h_n+\cdots)g_n\ . \tag{A7}$$

Only terms with even powers of δh_n contribute to the diagonal matrix elements of q_n, and only terms with odd powers of δh_n contribute to off-diagonal elements. Separate summation of these terms yields

$$q_n=w_n(g_n+g_n\delta h_ng_n)\ , \tag{A8}$$

where

$$w_n=[1-g_n\delta h_ng_n\delta h_n]^{-1} \tag{A9}$$

is diagonal. Furthermore, since

$$\langle\,n\,|\,g_n\delta h_ng_n\delta h_n\,|\,n\,\rangle\\ =\langle\,n\,|\,g_n\delta h_n\,|\,n+1\,\rangle\langle\,n+1\,|\,g_n\delta h_n\,|\,n\,\rangle\\ =\langle\,n+1\,|\,g_n\delta h_ng_n\delta h_n\,|\,n+1\,|\,\rangle\ , \tag{A10}$$

w_n may be treated as a scalar,

$$w_n=(1-[V^0(\alpha_n\alpha_{n+1})]^2/\{[z-\lambda(\alpha_n\alpha_{n+1})][z-\lambda(\alpha_{n+1}\alpha_n)]\})^{-1}\ . \tag{A11}$$

Equation (A6) can now be written as

$$t_n^0 = w_n(\tilde{G}^0)^{-1} g_n(1+\delta h_n g_n)\delta H_n \ . \tag{A12}$$

The matrix elements of t_n^0 are easily calculated from (A12) to give Eqs. (25) and (26).

APPENDIX B

Expressions for t_n^0 are given in (A1), (25), and (26). Each factor of $\tilde{G}^0$ in Eq. (29) is between two different t matrices t_{2n}^0 and t_{2n+1}^0. The only site on which both t_{2n}^0 and t_{2n+1}^0 have nonzero matrix elements is $2n+1$. Thus $\tilde{G}^0$ may be replaced by $|2n+1\rangle[z-\epsilon^0(\alpha_{2n+1})]^{-1}\langle 2n+1|$. Then separate summation of terms with even and odd powers of t^0 in (29) yields

$$\begin{aligned} t'_{2n} = \sum_{m=0,1} P_{\text{even}}(\{ & t_{2n+m}^0 + t_{2n+m}^0 \mid 2n+1\rangle[z-\epsilon^0(\alpha_{2n+1})]^{-1}\langle 2n+1 \mid t_{2n+1-m}^0 \mid 2n+1\rangle \\ & \times[z-\epsilon^0(\alpha_{2n+1})]^{-1} f_{2n}\langle 2n+1 \mid t_{2n+m}^0\} \\ & + t_{2n+m}^0 \mid 2n+1\rangle[z-\epsilon^0(\alpha_{2n+1})]^{-1} f_{2n}\langle 2n+1 \mid t_{2n+1-m}^0)\ , \end{aligned} \tag{B1}$$

where

$$\begin{aligned} f_{2n} &= \sum_{j=0}^{\infty} \{\langle 2n+1 \mid t_{2n+m} \mid 2n+1\rangle[z-\epsilon^0(\alpha_{2n+1})]^{-2}\langle 2n+1 \mid t_{2n+1-m} \mid 2n+1\rangle\}^j \\ &= \{1 - a^0(\alpha_{2n+1}\alpha_{2n}) a^0(\alpha_{2n+1}\alpha_{2n+2})[z-\epsilon^0(\alpha_{2n+1})]^{-2}\}^{-1} \end{aligned} \tag{B2}$$

is a scalar factor.

The matrix elements of t'_{2n} can now be calculated and configuration averaged over α_{2n+1} to give $t_{2n}^{(1)}$ in terms of renormalized a's and b's. Terms in (B1) with odd powers of t^0 contribute only to the diagonal elements of t'_{2n} while even terms in t^0 contribute to off-diagonal elements. Only one of the terms in the sum over m in (B1) is nonzero because $\langle 2n \mid t_{2n+1} = 0 = \langle 2n+2 \mid t_{2n}$. We find

$$\begin{aligned} a^{(1)}(\alpha_{2n},\alpha_{2n+2}) &= \langle a^0(\alpha_{2n}\alpha_{2n+1}) + [b^0(\alpha_{2n}\alpha_{2n+1})]^2 a^0(\alpha_{2n+1}\alpha_{2n+2}) \\ &\qquad \times[d^0(\alpha_{2n}\alpha_{2n+1}\alpha_{2n+2})]^{-1}\rangle_{\text{odd}}\ , \\ b^{(1)}(\alpha_{2n},\alpha_{2n+2}) &= \langle b^0(\alpha_{2n}\alpha_{2n+1}) b^0(\alpha_{2n+1}\alpha_{2n+2})[z-\epsilon^0(\alpha_{2n+1})] \\ &\qquad \times[d^0(\alpha_{2n}\alpha_{2n+1}\alpha_{2n+2}]^{-1}\rangle_{\text{odd}}\ , \end{aligned} \tag{B3}$$

where

$$d^0(\alpha\beta\gamma) = [z-\epsilon^0(\beta)]^2 - a^0(\beta\alpha)a^0(\beta\gamma)\ . \tag{B4}$$

With the use of the relations in Sec. II B, the configurational averages in (B3) are explicitly written as in (31).

---

*On sabbatical leave from Departamento de Fisica, Pontifícia Universidade Católica, Rio de Janeiro, Caixa Postal 38071, 20000 Rio de Janeiro, Brazil.

[1] *Physics in One Dimension,* edited by Y. Bernasconi and T. Schneider (Springer, Berlin, 1981) and references therein.

[2] J. J. Hopfield, Proc. Natl. Acad. Sci. U.S.A. 71, 3640 (1974).

[3] J. Hubbard, Phys. Rev. Lett. 3, 77 (1958); E. N. Economou and C. T. White, *ibid.* 38, 289 (1977); S. H. Liu, Phys. Rev. B 15, 4281 (1977).

[4] N. F. Mott and W. D. Twose, Adv. Phys. 10, 107 (1961).

[5] H. Matsuda and K. Ishii, Prog. Theor. Phys. Suppl. 45, 56 (1970).

[6] H. Matsuda, Prog. Theor. Phys. 36, 1070 (1966).

[7] J. E. Gubernatis and P. L. Taylor, J. Phys. C 6, 1889 (1973).

[8] H. Schmidt, Phys. Rev. 105, 425 (1957).

[9] P. Dean, Rev. Mod. Phys. 44, 127 (1972).

[10] L. Nordheim, Ann. Phys. (Leipzig) 9, 607 (1931); 9, 641

(1931).
[11]J. L. Beeby and S. F. Edwards, Proc. R. Soc. London Ser. A 274, 395 (1963).
[12]P. Soven, Phys. Rev. 156, 809 (1967); D. W. Taylor, *ibid.* 156, 1017 (1967).
[13]R. J. Elliott, J. A. Krumhansl, and P. L. Leath, Rev. Mod. Phys. 46, 465 (1974).
[14]H. Ehreinreich and L. M. Schwartz, in *Solid State Physics,* edited by H. Ehrenreich, F. Seitz, and D. Turnbull (Academic, New York, 1976), Vol. 31, p. 149.
[15]*Excitations in Disordered Systems,* edited by M. F. Thorpe (Plenum, New York, 1982), and references therein.
[16]C. T. White and E. N. Economou, Phys. Rev. B 15, 3742 (1977).
[17]J. Hubbard, Phys. Rev. B 19, 1828 (1979).
[18]T. Kaplan, P. L. Leath, L. J. Gray, and H. W. Diehl, Phys. Rev. B 21, 4230 (1980); L. J. Gray and T. Kaplan, *ibid.* 24, 1872 (1981).
[19]C. E. T. Gonçalves da Silva and B. Koiller, Solid State Commun. 40, 215 (1981).
[20]K. G. Wilson, Rev. Mod. Phys. 47, 773 (1975).
[21]B. Koiller, M. O. Robbins, M. A. Davidovich, and C. E. T. Gonçalves da Silva, Solid State Commun. 45, 955 (1983).
[22]C. E. T. Gonçalves da Silva and P. Schlottmann, Solid State Commun. 41, 819 (1982).
[23]P. Lloyd, J. Phys. C 2, 1717 (1969).
[24]S. D. Drell, M. Weinstein, and S. Yankelowicz, Phys. Rev. D 14, 1769 (1977); R. Jullien, J. N. Fields, and S. Doniach, Phys. Rev. B 16, 4889 (1977); J. E. Hirsch and J. V. José, *ibid.* 22, 5339 (1980); W. Hanke and J. E. Hirsch, *ibid.* 25, 6748 (1982).
[25]L. P. Kadanoff and A. Houghton, Phys. Rev. B 11, 377 (1975).
[26]M. O. Robbins and L. M. Falicov, Phys. Rev. B 25, 2343 (1982).
[27]F. Ducastelle and F. Cyrot-Lackmann, J. Phys. Chem. Solids 31, 1295 (1970).
[28]The number of moments reproduced by the ATA quoted here agrees with Ref. 14, p.203. The numbers is increased by one if the VCA is used to define $\tilde{H}$ in Eq. (17).
[29]J. A. Blackman, D. M. Esterling, and N. F. Berk, Phys. Rev. B 4, 2412 (1971).
[30]See for example W. H. Butler, Phys. Rev. B 8, 4499 (1973).
[31]This technique is equivalent to the negative eigenvalue method of Ref. 9.
[32]See, for example, L. P. Kadanoff, Rev. Mod. Phys. 49, 267 (1977).